Analytical Model Accuracy Requirements for Structural Dynamic Systems

Jay-Chung Chen*
Jet Propulsion Laboratory, California Institute of Technology, Pasadena, California

A test/analysis correlation criterion has been developed for the analytical model accuracy requirement for structural dynamic systems. It is based on the principle of equal errors from the model inaccuracy and the uncertainties of dynamic environments. The forcing functions are idealized to establish the base for uncertainty definition and the maximum allowable errors from these uncertainties are obtained. Then the model accuracy requirement is established by comparing the responses due to the model errors with those due to the forcing function uncertainties.

Nomenclature

f_0 = quasisteady state part of forcing function
f_1 = coefficient of periodic part of forcing function
$\{F(t)\}$ = forcing function vector
$\{G(t)\}$ = generalized forcing function vector
$[K_1]$ = launch vehicle stiffness matrix
$[K_{ij}]$ = partitioned stiffness matrix of the composite system
$[m_1]$ = launch vehicle mass matrix
$[m_2]$ = payload mass matrix
$[m_{rr}]$ = payload rigid-body mass
n = number of degrees of freedom
$\{q\}$ = generalized coordinates vector
u = displacement-like quantity
$\{x_1\}$ = launch vehicle degrees of freedom
$\{x_2\}$ = payload degrees of freedom
$\{x_e\}$ = payload elastic degrees of freedom
$\{x_I\}$ = launch vehicle/payload interface degrees of freedom
ϵ_f = allowable errors due to forcing function uncertainties
ϵ_m = errors due to model inaccuracy
$[\rho]$ = modal damping matrix
$[\phi]$ = eigenvector matrix
$[\phi_R]$ = rigid-body modes
Ω = forcing function frequency
$[\omega]$ = eigenvalue matrix

Introduction

DESIGNING a structure that will be able to survive a prescribed dynamic environment is generally accomplished today by using an analytical model of the structure. Since many structural systems will not be subjected to their design dynamic environments prior to their commission, it is very important that the analytical model be able to predict the behavior of the physical system quite accurately. Although advancements in modern analytical techniques and the ever-increasing capabilities in computer technology make it possible for engineers to model a physical system to any desired degree of accuracy, cost and schedule constraints preclude such an approach in the design process. Thus, an engineering model for the purpose of the design analysis process will always be an approximate representation of the physical system. The process gives rise to two important and fundamental questions: 1) "Given the dynamic environment with a known degree of accuracy, how accurate must the analytical model be in order to extract adequate information for the design?" 2) "Since the structure will not be subjected to the actual dynamic environment, to what criteria should the accuracy of the model be referred?" In the past these questions have not be addressed adequately.

For aerospace payload structural systems, where the responses and loads dictate the design and, thus, the size and weight of the structure, the accuracy of the analytical model is of major importance because of the stringent weight constraints. A so-called test-verified analytical model is always required for the final verification loads analysis. The modal test, from which the natural frequencies, mode shapes, modal damping, and other dynamic characteristics are determined experimentally, is used to verify the analytical model. The comparisons of various modal characteristics, such as the natural frequencies and mode shapes obtained from the modal test and its corresponding analytical predictions, define the accuracy of the analytical model. The criteria for test verification of an analytical model have never been defined clearly. Usually, a maximum allowable percentage error for the frequency comparison and maximum allowable off-diagonal terms for the orthogonality check will be required. Nevertheless, these are based more on an individual's experiences than on any rational derivations.

Furthermore, recent developments in the application of system identification to structural dynamic testing[1-3] enable the analyst to improve upon the model systematically by using the test results. New predictions are then made by the improved model and compared with the test results. This procedure is repeated until a "predetermined" convergence between analysis and test is achieved. Again, the criteria for the convergence are "predetermined" based on the individual's experiences rather than rigorous reason.

In the present study, an attempt is made to establish a criterion for the analytical model accuracy requirement which will be based on a rational procedure instead of an individual's experience or intuition.

Approach

The accuracy of analytical predictions is dependent on two aspects; one is the accuracy of the model itself and the other is the accuracy of the prescribed dynamic environments based on which responses and loads are calculated. The dynamic environments from which the external forcing functions are derived are usually measured from actual flights. The variations in amplitude and frequency content of the forcing

Presented as Paper 82-0734 at the AIAA/ASME/AHS 23rd Structures, Structural Dynamics and Materials Conference, New Orleans, La., May 10-12, 1982; submitted Sept. 14, 1982; revision received Aug. 2, 1983.

*Member of Technical Staff, Applied Mechanics Technology Section. Member AIAA.

function are usually large. However, only a few selected or synthesized forcing functions are applied in the loads analysis. Thus, inherently, the analytical predictions of responses and loads possess a built-in inaccuracy due to the variations in the applied forcing function. Analysts have no control over these inaccuracies since they are given quantities. On the other hand, model accuracy is controlled to a great extent by the analysts. Therefore, it is only natural that the most desirable model should produce at the most the same amount of errors as produced by the inaccuracies in the forcing functions.

The responses and loads used in the structural design process can be obtained by performing a transient analysis of the coupled payload and launch vehicle system analytical dynamic model. The combined dynamic model of the payload/launch vehicle is large and complex. Many different methods have been developed for computing the responses and loads.[4,5] In the present study emphasis will be placed on methods wherein the main objective is to obtain the payload responses and loads. The dynamic environments applied to the payload then will be in the form of payload/launch vehicle interface accelerations. The detailed derivation has been developed in previous studies.[6,7] Nevertheless, the governing equations will be examined briefly:

$$\begin{bmatrix} m_1 & 0 \\ 0 & m_2 \end{bmatrix} \begin{Bmatrix} \ddot{x}_1 \\ \ddot{x}_2 \end{Bmatrix} + \left(\begin{bmatrix} k_1 & 0 \\ 0 & 0 \end{bmatrix} + \begin{bmatrix} k_{11} & k_{21} \\ k_{12} & k_{22} \end{bmatrix} \right) \begin{Bmatrix} x_1 \\ x_2 \end{Bmatrix} = \begin{Bmatrix} F(t) \\ 0 \end{Bmatrix} \quad (1)$$

Equation (1) is the governing equation of the coupled composite system, where

$\{x_1\}$ = launch vehicle degrees of freedom (DOF)
$\{x_2\}$ = payload DOF
$[m_1]$ = mass matrix of the launch vehicle
$[m_2]$ = mass matrix of the payload
$[k_1]$ = stiffness matrix of the launch vehicle
$[k_{11}], [k_{12}], [k_{21}], [k_{22}]$ = submatrices of the total payload stiffness matrix partitioned into launch vehicle/payload interface DOF and payload DOF

Although damping is not included in Eq. (1), it will be incorporated later in the form of modal damping. Also, for simplicity, it will be assumed that the payload is supported in a statically determinate manner such that

$$[k_{11}] = [\phi_R]^T [k_{22}] [\phi_R]$$
$$[k_{21}] = -[\phi_R]^T [k_{22}] = [k_{12}]^T \quad (2)$$

where $[\phi_R]$ is the payload rigid-body transformation matrix defined as the payload displacement due to unit displacement of the launch vehicle/payload interface DOF, $\{x_I\}$; and $\{x_I\}$ the launch vehicle/payload interface DOF connecting payload to launch vehicle, a subset of the launch vehicle DOF $\{x_1\}$.

Next, the motion of the payload will be decomposed into two parts, namely, the rigid-body motion and the elastic motion.

$$\{x_2\} = [\phi_R]\{x_I\} + \{x_e\} \quad (3)$$

The first term on the right-hand side of Eq. (3) is the rigid-body motion. The second term, $\{x_e\}$, is the elastic motion or relative motion with reference to the interface. It should be noted that only the elastic motion $\{x_e\}$ will generate internal loads in the structure. Using Eqs. (2) and (3), Eq. (1) can be transformed into the following form:

$$\begin{bmatrix} m_1 + m_{rr} & \phi_R^T m_2 \\ m_2 \phi_R & m_2 \end{bmatrix} \begin{Bmatrix} \ddot{x}_I \\ \ddot{x}_e \end{Bmatrix} + \begin{bmatrix} k_1 & 0 \\ 0 & k_{22} \end{bmatrix} \begin{Bmatrix} x_I \\ x_e \end{Bmatrix} = \begin{Bmatrix} F(t) \\ 0 \end{Bmatrix} \quad (4)$$

where

$$[m_{rr}] = [\phi_R]^T [m_2] [\phi_R] \quad (5)$$

denoted as rigid-body mass.

From Eq. (4), the payload elastic DOF is governed by

$$[m_2]\{\ddot{x}_e\} + [k_{22}]\{x_e\} = -[m_2][\phi_R]\{\ddot{x}_I\} = -[m_2][\phi_R]\{\ddot{x}_I\} \quad (6)$$

Equation (6) indicates that the payload elastic response can be calculated once the interface acceleration $\{\ddot{x}_I\}$ has been determined.

Although Eq. (4) implies that the interface acceleration $\{\ddot{x}_I\}$ is a function of the payload dynamic characteristics, methods have been developed to obtain the proper interface acceleration from previously analyzed composite systems consisting of an identical launch vehicle and a different payload.[8] In the present study, Eq. (6) will be treated as the governing equation for the payload structural system. The left-hand side of Eq. (6) represents the analytical model constructed by the analysts; the right-hand side represents the prescribed external forcing function. Equation (6) will be rewritten as

$$[m]\{\ddot{x}\} + [k]\{x\} = \{F(t)\} \quad (7)$$

Clearly, the accuracy of the response $\{x\}$ prediction depends on how realistically the mass $[m]$, stiffness $[k]$, and external forcing function $\{F(t)\}$ simulate the physical system. In other words, the prediction errors are due to two sources: one from the modeling, namely, $[m]$ and $[k]$, and the other from the forcing function $\{F(t)\}$. As mentioned before, if one defines the errors due to $\{F(t)\}$ as the allowable errors, the accuracy requirement for modeling $[m]$ and $[k]$ will be that the errors due to $[m]$ and $[k]$ inaccuracies should be equal to or less than the allowable errors.

The left-hand side of Eq. (7) is also used in predicting the payload natural frequencies, normal modes, and other "dynamic characteristics." The results of the comparison between these analytically predicted dynamic characteristics and the corresponding modal test measured values will be used in the judgment of how accurate the predicted responses will be. A previous study[9] successfully has established the relationship between the errors in the natural frequencies and mode shapes and the predicted responses for the cases where the model errors are very small. However, the results are valid only for certain classes of forcing functions. Here, the effects of errors in frquency and mode shape prediction on the response prediction will be established first. Let

$$\{x\} = [\phi]\{q(t)\} \quad (8)$$

where $[\phi]$ is the normal mode matrix and $\{q\}$ is the generalized coordinate. Then Eq. (7) can be transformed into the following:

$$\{\ddot{q}\} + 2[\rho][\omega]\{\dot{q}\} + [\omega^2]\{q\} = \{G(t)\} \quad (9)$$

where $\{G(t)\}=[\phi]^T\{F(t)\}$ is the generalized forcing function, $\lceil\rho\rfloor$ the percentage of modal damping, and $\lceil\omega\rfloor$ the natural frequency matrix. The errors in $\lceil\omega\rfloor$ affect the calculation of $\{q(t)\}$ and thus $\{x(t)\}$.

Next, the responses for the correct model case, the forcing function deviation case, and the modeling error case will be calculated. Let

$\{F(t)\}$ = forcing functions for the design
$\{\bar{F}(t)\}$ = typical forcing function deviation
$[\phi]_A$ = analytically predicted normal mode matrix
$[\phi]_T$ = test measured normal mode matrix
$[\omega]_A$ = frequency matrix from the analytical model
$[\omega]_T$ = test measured frequency matrix for the correct model case

For the correct model case,

$$\{x\}=[\phi]_T\{q_T\}\{\ddot{q}_T\}+2[\rho][\omega]_T\{\dot{q}_T\}+[\omega^2]_T\{q_T\}$$
$$=[\phi]_T^T\{F(t)\}=\{G(t)\} \tag{10}$$

For the forcing function deviation case,

$$\{\bar{x}\}=[\phi]_T\{\bar{q}\}\{\ddot{\bar{q}}\}+2[\rho][\omega]_T\{\dot{\bar{q}}\}+[\omega^2]_T\{\bar{q}\}$$
$$=[\phi]_T^T\{\bar{F}(t)\}=\{\bar{G}(t)\} \tag{11}$$

For the model error case,

$$\{x_0\}=[\phi]_A\{q_0\}\{\ddot{q}_0\}+2[\rho][\omega]_A\{\dot{q}_0\}$$
$$+[\omega^2]_A\{q_0\}=[\phi]_A^T\{F(t)\}=\{G_0(t)\} \tag{12}$$

The differences between $\{\bar{x}\}$ and $\{x\}$ and $\{x_0\}$ and $\{x\}$ should provide some direct indications about the allowable errors and the errors due to modeling inaccuracy, respectively. But these response differences in the form of displacements are not only functions of time but are vectors also. Therefore, scalar quantities will be defined for the purpose of convenient, yet meaningful, comparisons.

The allowable error will be defined as

$$\epsilon_f(t)=\sum_{i=1}^{n}(m_T)_i|\bar{x}_i^2-x_i^2|=(m_T)_1|\bar{x}_1^2-x_1^2|$$
$$+(m_T)_2|\bar{x}_2^2-x_2^2|+\cdots+(m_T)_n|\bar{x}_n^2-x_n^2| \tag{13}$$

where $(m_T)_i$ is an element in the true or correct mass matrix $[m]_T$ associated with the ith DOF. One may look at Eq. (13) as the summation of the response square differences weighted by the amount of mass associated with that DOF. Hence, the response differences for those DOF with larger mass are more important than those with smaller mass. This is certainly physically meaningful and represents the difference of the length of the two vectors mathematically. Also, Eq. (13) can be looked at as the differences between local kinetic energy types associated with each DOF.

$$(m_T)_1(\bar{x}_1^2-x_1^2)+(m_T)_2(\bar{x}_2^2-x_2^2)+\cdots+(m_T)_n(\bar{x}_n^2-x_n^2)$$
$$=\{\bar{x}\}^T[m]_T\{\bar{x}\}-\{x\}^T[m]_T\{x\}$$
$$=\{\bar{q}\}^T[\phi]_T^T[m]_T[\phi]_T\{\bar{q}\}-\{q_T\}^T[\phi]_T[m]_T[\phi]_T\{q_T\}$$
$$=\{\bar{q}\}^T\{\bar{q}\}-\{q_T\}^T\{q_T\}=[\bar{q}_1^2-(q_T)_1^2]$$
$$+[\bar{q}_2^2-(q_T)_2^2]+\cdots+[\bar{q}_n^2-(q_T)_n^T] \tag{14}$$

Note that

$$[\phi]_T^T[m]_T[\phi]_T=[I]=\text{unity matrix} \tag{15}$$

Equation (15) states that the measured normal modes matrix is orthogonal with respect to the true mass matrix which, incidentally, will not be required for computing ϵ_f. Then,

$$\epsilon_f(t)=(m_T)_1|\bar{x}_1^2-x_1^2|+(m_T)_2|\bar{x}_2^2-x_2^2|$$
$$+\cdots+(m_T)_n|\bar{x}_n^2-x_n^2|\cong|\bar{q}_1^2-(q_T)_1^2|+|\bar{q}_2^2-(q_T)_2^2|$$
$$+\cdots+|\bar{q}_n^2-(q_T)_n^2|=\sum_{i=1}^{n}|\bar{q}_i^2-(q_T)_i^2| \tag{16}$$

where n is the number of generalized coordinates. It should be noted that the allowable error ϵ_f is a function of time t.

Next, the error due to model accuracy will be defined as

$$\epsilon_m(t)=\sum_{i=1}^{n}m_i|(x_0)_i^2-x_i^2|=m_1|(x_0)_1^2-x_1^2|$$
$$+m_2|(x_0)_2^2-x_2^2|+\cdots+m_n|(x_0)_n^2-x_n^2| \tag{17}$$

where m_i is an element in the analytical mass matrix $[m]$ associated with the ith DOF. Similar physical meanings can be applied to ϵ_m such as those of Eq. (13) for ϵ_f.

$$m_1[(x_0)_1^2-x_1^2]+m_2[(x_0)_2^2-x_2^2]+\cdots+m_n[(x_0)_n^2-x_n^2]$$
$$=\{x_0\}^T[m]\{x_0\}-\{x\}^T[m]\{x\}=\{q_0\}^T[\phi]_A^T[m][\phi]_A\{q_0\}$$
$$-\{q_T\}^T[\phi]_T^T[m][\phi]_T^T\{q_T\}=\{q_0\}^T\{q_0\}-\{q_T\}^T\{q_T\}$$
$$-\{q_T\}^T[\Delta M]\{q_T\}=[(q_0)_1^2-(q_T)_1^2]+[(q_0)_2^2-(q_T)_2^2]$$
$$+\cdots+[(q_0)_n^2-(q_T)_n^2]-2\sum_{i=1}^{n}\sum_{j=1}^{n}\Delta M_{ij}(q_0)_i(q_T)_j$$
$$\text{for } i\neq j \tag{18}$$

Note that

$$[\phi]_A^T[m][\phi]_A=[I]$$
$$(\phi]_T^T[m][\phi]_T=\text{orthogonality check}=[I]+[\Delta M] \tag{19}$$

where $[\Delta M]$ contains the usually small off-diagonal terms from the orthogonality check.

$$\epsilon_m(t)\cong|(q_0)_1^2-(q_T)_1^2|+|(q_0)_2^2-(q_T)_2^2|$$
$$+\cdots+|(q_0)_n^2-(q_T)_n^2|+2\sum_{i=1}^{n}\sum_{j=1}^{n}|\Delta M_{ij}(q_0)_i(q_T)_j|$$
$$\text{for } i\neq j \tag{20}$$

In an overall sense, ϵ_f and ϵ_m represent the errors due to the forcing function and model inaccuracy, respectively. At the conclusion of the modal test, $[\phi]_A$ and $[\phi]_T$, the frequencies $[\ \omega\ ]_A$ and $[\ \omega\ ]_T$, and the resulting orthogonality check having been determined, ϵ_f and ϵ_m can be computed. If the results satisfy the following inequality,

$$\epsilon_m(t)\leq\epsilon_f(t)\quad\text{for all}\quad t \tag{21}$$

then the model will be considered to be sufficiently accurate to predict the responses within the allowable errors.

The effects of mode shape and frequency correlation on the response prediction are different for each mode. Depending on the forcing function, some modes play a more important role than others. These modes are also important if one

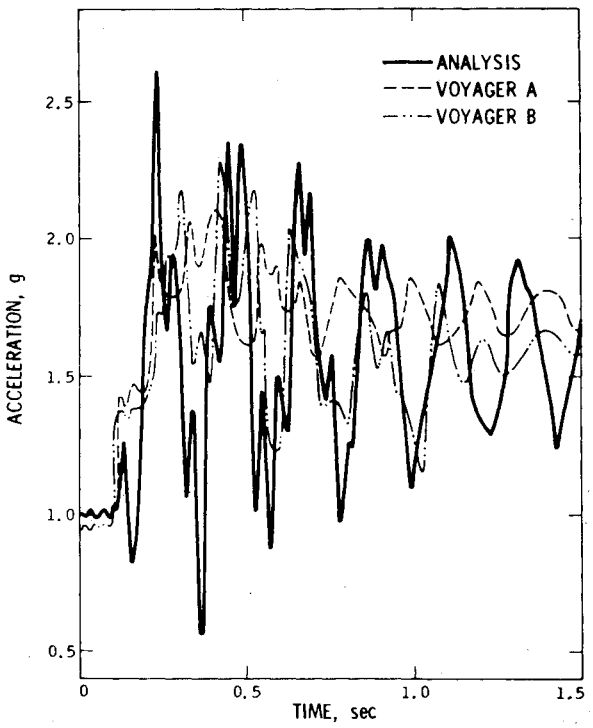

Fig. 1 Interface acceleration for launch.

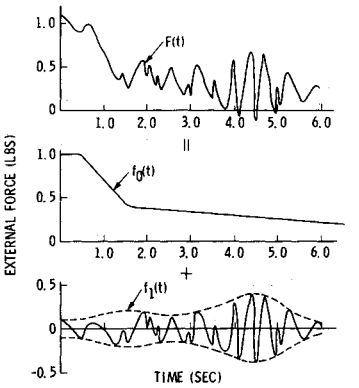

Fig. 2 Forcing function decomposition.

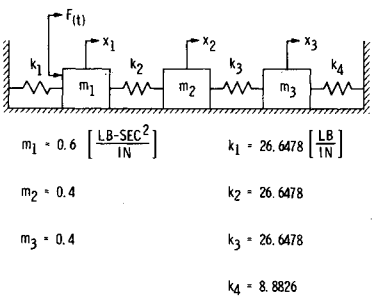

Fig. 3 Sample problem.

desires to modify the model to improve the prediction. From Eq. (20), it becomes clear that by comparing the ϵ_m value with each individual term on the right-hand side, the predominant modes for the response prediction readily can be identified. This is a very significant step in the system identification application for model updating using test results.

Transient Envelope Solution

Another aspect of the above procedure is that the solutions of the modal responses or generalized coordinates are expressed by Eqs. (10-12). It seems that a system transient solution must be performed to obtain the proper results. This would be a costly and time-consuming procedure. Figure 1 shows the payload/launch vehicle interface accelerations of the Voyager spacecraft, wherein both the flight-measured data and the corresponding analytical prediction are included. First, the transient signal consists of a steady-state signal superimposed on a periodic signal with varying amplitude and frequency. Second, the measured data, as well as the analytical predictions, have phase differences which place their peaks at different time points. Therefore, if these data are to be used in the design, the maximum values of the singals should be selected, instead of values at any particular time. In other words, it is the envelope of the peaks that is of interest instead of the actual transient solution. A method now will be developed to obtain the transient envelopes in a cost-effective manner.

Without loss of generality, Eqs. (10-12) can be represented by

$$\ddot{u}+2\rho\omega\dot{u}+\omega^2 u=F(t) \tag{22}$$

where the external forcing function $F(t)$ is shown in Fig. 2. $F(t)$ can be decomposed as

$$F(t)=f_0(t)+f_1(t)\cos\Omega t \tag{23}$$

where Ω itself is a time-varying function.

The $f_0(t)$, $f_1(t)$, and Ω are varying slowly with respect to time, but the product of $f_1(t)\cos\Omega t$ is a rapid time-varying function. The solution of Eq. (22) can be expressed approximately as

$$u(t)\cong u_0(t)+u_1(t) \tag{24}$$

where

$$\omega^2 u_0 \simeq f_0(t) \quad \text{and} \quad \ddot{u}_1+2\rho\omega\dot{u}_1+\omega^2 u_1=f_1(t)\cos\Omega t \tag{25}$$

The $u_0(t)$ is basically an approximation static solution which is valid only if the part of the forcing function signal is, indeed, very slowly varying with respect to time. Let

$$u_1(t)=A(t)\cos\Omega t+B(t)\sin\Omega t \tag{26}$$

The amplitudes $A(t)$ and $B(t)$ can be obtained by solving the following equations:

$$\frac{dA}{dt}+\rho\omega A-\left(\frac{\omega^2-\Omega^2}{2\Omega}\right)B=0$$

$$\frac{dB}{dt}+\rho\omega B+\left(\frac{\omega^2-\Omega^2}{2\Omega}\right)A=\frac{f_1(t)}{2\Omega} \tag{27}$$

The detailed derivation can be found in the Appendix. Equation (26) can be written as

$$u_1(t)=a(t)\cos[\Omega t-\phi(t)] \tag{28}$$

where

$$a(t)=[A^2(t)+B^2(t)]^{1/2}, \quad \tan\phi=B/A \tag{29}$$

Clearly, $A(t)$ is a slowly varying envelope of $u_1(t)$. The upper and lower bounds of the solution will be

$$u(t)\,|_{\text{upper}}=\frac{1}{\omega^2}f_0(t)+a(t)$$

$$u(t)\,|_{\text{lower}}=\frac{1}{\omega^2}f_0(t)-a(t) \tag{30}$$

Table 1 Dynamic characteristics from test and analysis

	First mode		Second mode		Third mode	
	Test	Analysis	Test	Analysis	Test	Analysis
Natural frequeny, rad/s	4.713	3.534	9.425	8.987	14.137	13.983
Mode shape						
x_1,	0.667	0.472	1.000	1.000	−0.400	−0.417
x_2	1.000	0.812	0	0.182	1.000	1.000
x_3	1.000	1.000	−1.000	−0.857	−0.600	−0.517
Kinetic energy						
x_1	25.0	16.78	60.0	66.16	15.0	17.0
x_2	37.5	33.09	0	1.46	62.5	65.5
x_3	37.5	50.13	40.0	32.4	22.5	17.5

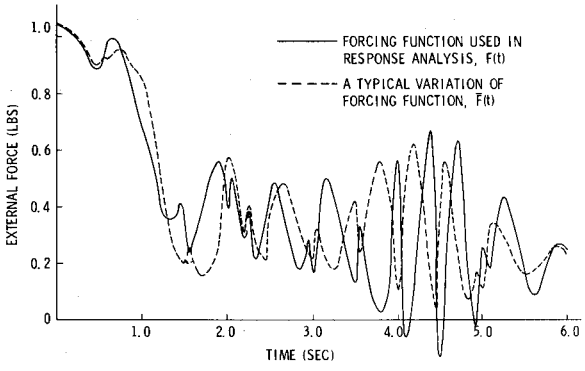

Fig. 4 Dynamic environments.

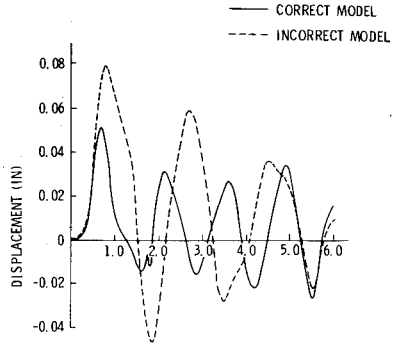

Fig. 5 x_3 comparison for model variation.

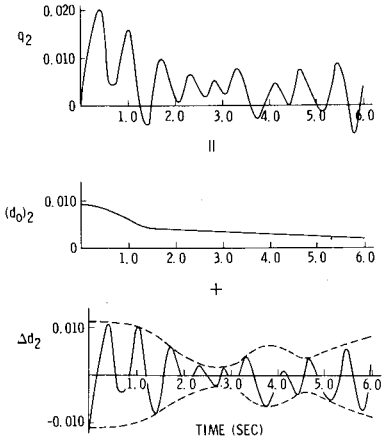

Fig. 6 Transient envelope solution.

Table 2 Test/analysis error comparison

	First mode	Second mode	Third mode	Average
Natural frequency error, %	25	4.65	1.09	10.25
Mode shape rss error	0.27	0.23	0.085	0.195
Kinetic energy distribution rss error, %	15.7	9.88	5.12	10.23

These upper and lower bounds are much more meaningful than the individual peaks in the response comparison, since no phase matching problem exists. Also, because of the slow varying in time, a much larger time interval can be used to calculate the numerical solutions for Eq. (27). This makes the procedure more cost effective.

Sample Problem

The proposed procedure will be demonstrated using a sample problem as shown in Fig. 3. The governing equation for this 3-DOF system is as follows:

$$\begin{bmatrix} m_1 & 0 & 0 \\ 0 & m_2 & 0 \\ 0 & 0 & m_3 \end{bmatrix} \begin{Bmatrix} \ddot{x}_1 \\ \ddot{x}_2 \\ \ddot{x}_3 \end{Bmatrix} + \begin{bmatrix} k_1+k_2 & -k_2 & 0 \\ -k_2 & k_2+k_3 & -k_3 \\ 0 & -k_3 & k_3+k_4 \end{bmatrix} \begin{Bmatrix} x_1 \\ x_2 \\ x_3 \end{Bmatrix} = \begin{Bmatrix} F(t) \\ 0 \\ 0 \end{Bmatrix} \tag{31}$$

The nominal external forcing function $F(t)$ and its typical deviation $\bar{F}(t)$ are shown in Fig. 4. It will be assumed that the analyst made a mistake during modeling by letting $k_4=0$. The eigendata of Eq. (31) will be used as the test-measured data and the corresponding values with $k_4=0$ will be used as the analytical predictions. Table 1 lists the test and analysis natural frequencies and mode shapes together with the kinetic energy distribution. Although the modeling error consists of a

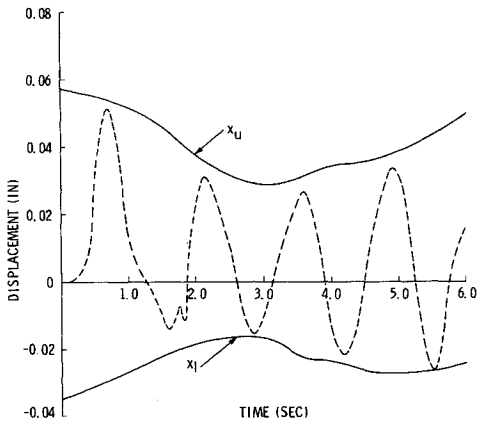

Fig. 7 x_3 response envelope.

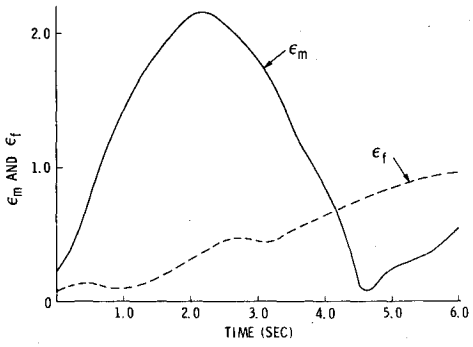

Fig. 8 Normalized kinetic energy difference.

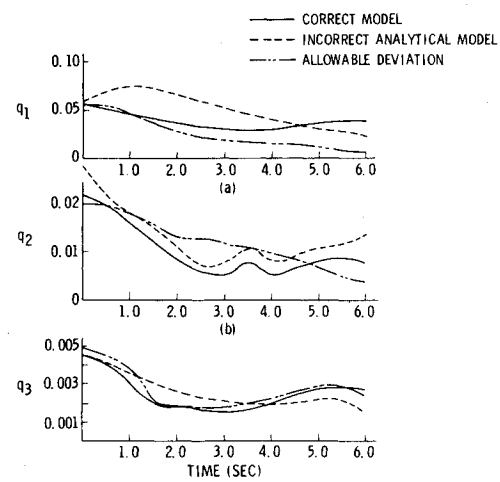

Fig. 9 Modal response envelopes.

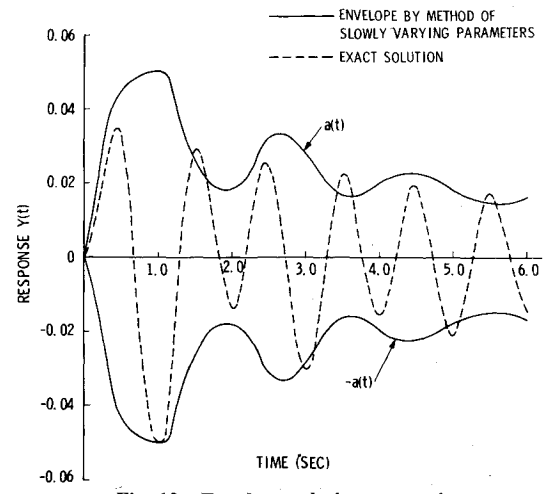

Fig. 10 Envelope solution comparison.

missing spring which is only one-third the stiffness of the other three springs, a noticeable difference in the eigendata can be observed. Table 2 shows the errors in the eigendata and the kinetic energy distribution. Despite the noticeable errors, it is not uncommon for similar errors to be found in realistic cases. Another correlation is the orthogonality check, in which the analytical mass matrix is pre- and postmultiplied by the test modes, as shown in Eq. (19). Since no modeling error is involved in the anlytical mass matrix, the orthogonality check will be perfect, i.e., resulting in a unity matrix. Many analysts would take this fact as a strong indication that the analytical model is, indeed, representing the physical system very closely.

The response of the x_3 DOF, when the system is subjected to the nominal forcing function using the correct model and the analysts' incorrect model, respectively, is calculated and shown in Fig. 5. The peak response of the incorrect model is 60% higher than the correct value. In view of the modal test/analysis comparison, which indicates an average 10% error in frequencies, 20% RSS error in the mode shapes, and 10% RSS error in the kinetic energy distribution, the 60% error in the displacement response seems surprisingly high. This, again, emphasizes the fact that model test/analysis correlation alone cannot demonstrate the model accuracy adequately.

Using the analytically predicted and test-measured frequencies and mode shapes, the modal responses for the various cases expressed by Eqs. (10-12) can be obtained. Figure 6 shows the second modal response of Eq. (10) with 5% modal damping for all cases. The envelope solution is compared with the transient solution. The upper and lower bounds of the physical response then can be calculated from the envelope solution of modal responses (Fig. 7 is a typical example). Again, the envelope and transient solutions are compared. Also, the allowable error ϵ_f and model error ϵ_m, as expressed by Eqs. (16) and (20), can be calculated using the proper modal responses and the orthogonality check. The result shown in Fig. 8 indicates that the model error are greater than the allowable error for $t<4.0$ s. In order to reduce the model error ϵ_m, the analytical model will have to be modified. By examining the model test/analysis correlation, as shown in Tables 1 and 2, one can see that the first mode is the one that should be improved, but the amount of improvement required is not indicated.

From Eqs. (16) and (20) it becomes clear that the discrepancy of each individual modal response comparison has a direct effect on the model error and the allowable error. Figure 9 shows the comparisons of modal response envelopes for the three cases. From these comparisons, the amount of improvement required to satisfy the criterion as shown in Eq. (21) can be readily quantified. Figure 9 clearly indicates that the major contributor to the modeling error is the first modal response q_1 for $t<4.0$. If one wants to improve the model by using the modal test resules, the emphasis for the correlations should be on the first mode. As to the other modes, their contributions are an order of magnitude smaller. Using this comparison, the amounts of change required to improve the modeling error ϵ_m can be used as the predetermined value for the convergence criterion in the system identification process.

Concluding Remarks

One important observation, which has been pointed out in attempting to answer the question of how accurate an

analytical model should be, is that the test/analysis comparison of the model characteristics such as frequencies and mode shapes is not adequate to judge the modeling accuracy. Since the errors of the response and loads are the subject of the accuracy requirement, accuracy of the forcing functions is to be considered also. A simple, but meaningful, method to obtain the transient envelope solution has been outlined, from which the upper and lower bounds of the responses can be obtained. The proposed accuracy requirement criterion is based on comparising the allowable and modeling errors in a rational yet simple approach in which the envelope solutions of the modal response have been applied. Although encouraging results were obtained using the sample problem, its adaptation to realistic space structures needs further study.

Appendix: Method of Slowly Varying Parameters

This method is also known as the method of Bogoliuboff and Mitropolski[10] and has been used to solve nonlinear vibration problems. For a given differential equation,

$$\frac{d^2x}{dt^2}+\sigma\frac{dx}{dt}+\alpha x=F(t)\cos\Omega t \tag{A1}$$

the solution will be assumed to be

$$x(t)=a(t)\cos[\Omega t-\phi(t)] \tag{A2}$$

where $F(t)$, $A(t)$, and $\phi(t)$ are slowly varying with respect to time.

Let

$$\theta(t)=\Omega t-\phi(t) \tag{A3}$$

Then

$$\frac{dx}{dt}=-a\Omega\sin\theta+a\frac{d\phi}{dt}\sin\theta+\frac{da}{dt}\cos\theta \tag{A4}$$

Since $a(t)$ and $\phi(t)$ are slowly varying, da/dt *and* $d\phi/dt$ are small; therefore, let

$$\frac{dx}{dt}=-a\Omega\sin\theta \tag{A5}$$

$$\frac{da}{dt}\cos\theta+a\frac{d\phi}{dt}\sin\theta=0 \tag{A6}$$

and

$$\frac{d^2x}{dt^2}=-a\Omega^2\cos\theta-\frac{da}{dt}\Omega\sin\theta+a\Omega\frac{d\phi}{dt}\cos\theta \tag{A7}$$

Upon substitution into Eq. (A1), one obtains

$$-a\Omega^2\cos\theta-\frac{da}{dt}\Omega\sin\theta+a\Omega\frac{d\phi}{dt}\cos\theta+f(a,\theta)=F(t)\cos\Omega t \tag{A8}$$

where

$$f(a,\theta)=\sigma\frac{dx}{dt}+\alpha x=-\sigma a\Omega\sin\theta+\alpha a\cos\theta \tag{A9}$$

Multiplying Eq. (A6) by $\Omega\sin\theta$, and Eq. (A8) by $\cos\theta$, and adding the results, will give

$$a\Omega\frac{d\phi}{dt}-a\Omega^2\cos^2\theta+f(a,\theta)\cos\theta=F(t)\cos(\theta+\phi)\cos\theta \tag{A10}$$

If $a(t)$, $\phi(t)$, and $F(t)$ are slowly varying functions, one may postulate that they remain constant over one cycle of $\theta(t)$. Then an averaging procedure will be performed as

$$\frac{1}{2\pi}\int_0^{2\pi}[\text{Eq. (A10)}]\,d\theta=0$$

which gives

$$2\Omega\bar{a}\frac{d\bar{\phi}}{dt}+(\alpha-\Omega^2)\bar{a}=\bar{F}\cos\bar{\phi} \tag{A11}$$

Similarly, multiplying Eq. (A6) by $\Omega\cos\theta$, and Eq. (A8) by $\sin\theta$, subtracting the results, and taking the average, gives

$$2\Omega\frac{d\bar{a}}{dt}+\sigma\Omega\bar{a}=\bar{F}\sin\bar{\phi} \tag{A12}$$

where the bar denotes an average value over one cycle.

Next, another transformation will be performed by Eq. (A11)$\times\cos\bar{\phi}$+Eq. (A12)$\times\sin\bar{\phi}$ and Eq. (A12)$\times\cos\bar{\phi}$−Eq. (A11)$\times\sin\bar{\phi}$. The resulting equations are

$$\begin{aligned}&\frac{dA}{dt}+\frac{\sigma}{2}A-\frac{(\alpha-\Omega^2)}{2\Omega}B=0\\&\frac{dB}{dt}+\frac{\sigma}{2}B+\frac{(\alpha-\Omega^2)}{2\Omega}A=\frac{F(t)}{2\Omega}\end{aligned} \tag{A13}$$

where

$$A(t)=\bar{a}\cos\bar{\phi}\quad\text{and}\quad B(t)=\bar{a}\sin\bar{\phi} \tag{A14}$$

Note that in Eq. (A13) the bar has been neglected. Substituting Eq. (A14) into Eq. (A2), one obtains

$$x(t)=A(t)\cos\Omega t+B(t)\sin\Omega t \tag{A15}$$

The envelope of $x(t)$ noted as $EN[x(t)]$ will be

$$En[x(t)]=[A^2(t)+B^2(t)]^{1/2}=a(t) \tag{A16}$$

Since $F(t)$ is a slowly varying function, the solutions of $A(t)$ and $B(t)$ are also slowly varying with respect to time. Therefore, a much larger integration interval can be taken during the computation.

A sample problem with the following parameters,

$$\sigma=2\rho\omega,\quad\alpha=\omega^2,\quad\rho=0.02,\quad\omega=2\pi$$

$$F(t)=e^{-\gamma t},\quad\gamma=0.05,\quad\Omega=\pi$$

$$x=\frac{dx}{dt}=0,\quad\text{at}\quad t=0$$

is solved to demonstrate the method. The result is plotted in Fig. 10, together with the exact solution. The envelope, obtained by the method of slowly varying parameters, does contain the peaks of the exact transient solution very nicely. In this particular example, the time interval used in the envelope solution is ten times that of the exact solution.

Acknowledgments

The research in this publication was carried out under the auspices of the Applied Mechanics Division of the Jet Propulsion Laboratory, California Institute of Technology, under NASA Contract NAS 7-100. The effort was supported by Samuel L. Venneri, Materials and Structures Division, NASA Office of Aeronautics and Space Technology.

References

[1]Pilkey, W.D. and Cohen, R., eds., "System Identification of Vibrating Structures, Mathematical Models from Test Data," American Society of Mechanical Engineers, New York, 1972.

[2]Collins, J.D., Hart, G.C., Hasselman, T.K., and Kennedy, B., "Model Optimization Using Statistical Estimation," J.H. Wiggins Co., Redondo Beach, Calif., Tech. Rept. 1087-2, May 1973.

[3]Chen, J.C. and Garba, J.A., "Analytical Model Improvement Using Modal Test Results," *AIAA Journal,* Vol. 18, June 1980, pp. 684-690.

[4]Ryan, R.S., Bullock, T., Holland, W.B., Kross, D.A., and Kiefling, L.A., "System Analysis Approach to Deriving Design Criteria (Loads) for Space Shuttle and Its Payloads," Vols. I and II, NASA TP 1950, Dec. 1981.

[5]Chen, J.C., Garba, J.A., Salama, M., and Trubert, M., *A Survey of Load Methodologies for Shuttle Orbiter Payloads,* Jet Propulsion Laboratory, California Institute of Technology, Pasadena, Calif., JPL Pub. 80-37, June 15, 1980.

[6]Chen, J.C., Wada, B.K., and Garba, J.A., "Launch Vehicle Payload Interface Response," *Journal of Spacecraft and Rockets,* Vol. 15, Jan.-Feb. 1978, pp. 7-11.

[7]Chen, J.C., Garba, J.A., and Wada, B.K., "Estimation of Payload Loads Using Rigid-Body Interface Acceleration," *Journal of Spacecraft and Rockets,* Vol. 16, March-April 1979, pp. 74-80.

[8]Chen, J.C., Zagzebski, K.P., and Garba, J.A., "Recovered Transient Load Analysis for Payload Structural Systems," *Journal of Spacecraft and Rockets,* Vol. 18, July-Aug. 1981, pp. 374-379.

[9]Chen, J.C. and Wada, B.K., "Criteria for Analysis-Test Correlation of Structural Dynamic Systems," *Journal of Applied Mechanics,* Vol. 42, No. 2, June 1975, pp. 471-477.

[10]Bogoliuboff, N.N. and Mitropolski, *Asymptotic Methods in the Theory of Non-Linear Oscillation,* Hindustan Publishing Col., 1961.